ARMY RESEARCH LABORATORY

Mutual Inductance Between a Coil and an Electromagnetically Launched Plate

by Charles R. Hummer
and Paul R. Berning

ARL-TR-1643 March 1998

The findings in this report are not to be construed as an official Department of the Army position unless so designated by other authorized documents.

Citation of manufacturer's or trade names does not constitute an official endorsement or approval of the use thereof.

Destroy this report when it is no longer needed. Do not return it to the originator.

Army Research Laboratory
Aberdeen Proving Ground, MD 21005-5066

ARL-TR-1643 **March 1998**

Mutual Inductance Between a Coil and an Electromagnetically Launched Plate

Charles R. Hummer, Paul R. Berning
Weapons and Materials Research Directorate, ARL

Abstract

A possible countermunition against kinetic energy (KE) rods is a thin square metal launched edge-on so that an edge strikes the rod first followed by the rest of the plate. A properly designed coil gun can launch plates edge-on to velocities of several hundred meters per second. The proper design of the coil gun depends on knowing the mutual inductance between the coil and the plate, which was calculated by assuming that the current distribution in plate can be described by a polynomial that has some arbitrary coefficients. These coefficients were determined by equating the magnetic induction of the current distribution to the negative of the applied magnetic induction of the launch coil at selected points on the plate. This step was aided by the fact that all the integrals arising from the Biot-Savart law are analytic. In the next step, the mutual inductance was calculated from the current distribution and the applied magnetic induction. The calculation was repeated for various plate positions in the coil. These results were used to design the power supply for the launch coil and to calculate the final velocity of the plate.

Table of Contents

INTENTIONALLY LEFT BLANK.

List of Figures

INTENTIONALLY LEFT BLANK.

1. Introduction

In previous work in the area of plate-rod interactions, such as in reactive armor [1] and momentum transfer armor (MTA) [2, 3], explosives were used to launch the plates with a velocity in the direction that is normal to the plane of the plate (face-on launch). Launching the plate with a velocity in the direction that is in the plane of the plate (edge-on launch) was not considered, because a substantial amount of explosive materials would be needed behind a small surface area of the plate, and confinement of the high-pressure gases would be difficult. There is some evidence, however, that plates launched edge-on may be more effective at defeating a kinetic energy (KE) rod. Both Hull code calculations [4, 5] and an experiment that simulated plates flying edge-on by firing a yawed projectile against a stationary target plate set at an angle [6] suggest a preference for edge-on orientation. This was confirmed in a series of experiments [7] where plates were launched, nonexplosively, by an electromagnetic (EM) launcher and intercepted a subscale rod. There are other advantages as well. A plate launched edge-on may be in an aerodynamically preferable orientation that can fly the distances required for some applications, and EM launchers do not have the special logistics and handling difficulties that are required for explosives. Because of these advantages, they appear to be a viable option and warrant continued examination. Accordingly, this launch option for KE threats is being studied at the U.S. Army Research Laboratory (ARL).

An EM launcher, which is well suited for edge-on launch of plates, is the reconnection gun, a type of coil gun invented by Cowan [8]. In this launcher, a time varying magnetic induction produced in an external launch coil induces a current in the plate to be launched. This action is similar to that of a transformer where the primary winding, the external launch coil, induces a current in the secondary winding, the plate. The force between the induced current and the external magnetic induction accelerates the plate out of the coil. Cowan and colleagues [9] demonstrated that high velocities can be achieved by using a number of external coils arranged in-line along a path. As a plate was passing through a coil, a current pulse was delivered at the proper time to accelerate the plate toward the next coil. This resulted in the launching of a 150-g aluminum plate to a velocity of 1.0 km/s. Although this multistage launcher did not use explosives, its use in nonenergetic momentum transfer armor (NEMTA) is probably not practical because of its size and weight. Therefore, only single-stage launchers are considered here.

2. Single-Stage Coil Guns

The electrical schematic of a single-stage coil gun [10] (Figure 1) is very similar to a series LRC circuit. Unlike the classic LRC circuit, the inductance associated with the launcher depends on the position of the plate within the coil. This dependence is due to the distribution of the magnetic induction in the core of the coil and around the plate. The resistor in this figure is not a physical resistor. It represents the energy losses within the system that may also vary with time, but it is usually assumed to be constant for the purposes of modeling.

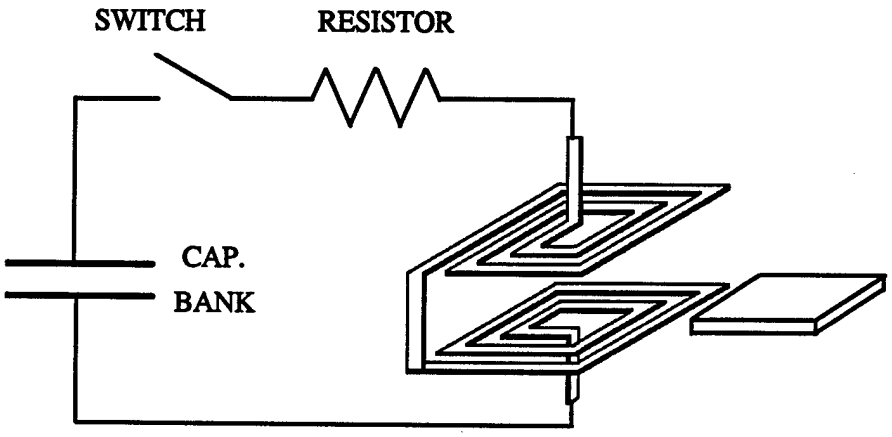

Figure 1. Schematic of a Single-Stage Coil Gun.

In designing a coil gun for the best performance, it is necessary to calculate the current through the coil, the plate's velocity, and the plate's position in the coil. These calculations require that the inductance of the coil, and its gradient, be known as functions of the plate's position. The coil's inductance is necessary to calculate the coil's current, and the inductance gradient is necessary to calculate the acceleration of the plate. Previously, models of proposed launch coil designs were made out of aluminum, then their inductances were measured with a Hewlett-Packard model 4263A LRC meter. This meter supplies an alternating voltage to the coil and analyzes the amplitude and phase of the current through the coil to determine its inductance. The results are digitally displayed on the meter and recorded for each plate position. These data are then used to estimate the inductance gradients. This study was tedious because of the number of coils that had to be constructed and measured. If it were possible to easily calculate the inductance and the gradient of

these coils, then a more complete study of various coils with different design parameters and geometries could have been performed. This report presents a method to calculate these quantities.

To illustrate the change in the distribution of the magnetic induction when a conductor is present, Figure 2 shows the result of a simple two-dimensional calculation [10]. The shaded area represents an aluminum plate in an oscillating magnetic induction, produced by two infinite current sheets, located at the thick solid lines to the left and to the right of the aluminum plate. Current in these sheets is equal in magnitude, but opposite in direction at all times. The total magnetic induction produced by these current sheets and the eddy current in the plate is shown as streamlines, located between the current sheets. The direction of the magnetic induction is tangent to these lines, and the magnitude is inversely proportional to the distance between neighboring lines. Because the magnetic induction produced by the eddy current tends to be equal, but opposite to the magnetic induction of the current sheets, their sum is small inside the aluminum plate, except at the left and right edges where the streamlines may enter the plate. Thus, the streamlines are bent around the aluminum plate. This bending of the streamlines concentrates them in the gap between the back edge of the plate and the left current sheet, indicating an area where there is a large magnetic induction and force on the plate. This force pushes the plate through the slot in the current sheets to the right and out of the coil. As the plate moves out, the streamlines straighten out and eventually become evenly spaced vertical lines, when the plate is completely out of the coil. The shape of the streamlines and the force on the plate can be easily calculated for this two-dimensional geometry. Unfortunately, two-dimensional calculations are not adequate, as has been demonstrated by another more detailed two-dimensional calculation [11], where the force on the plate for a transient current in the sheets and the heating effects in the plate were included. The plate velocity was calculated to be 140 m/s, but the experimental velocity was only 92 m/s. There was better agreement when an "effective 3-D correction factor" was introduced.

3. Eddy Currents

Three-dimensional eddy current calculations [12] are important in electrical engineering, and many publications are available on this subject. Most of these calculations can be divided into two broad categories. The first category is the quasi-stationary [13] problem, where the magnetic field

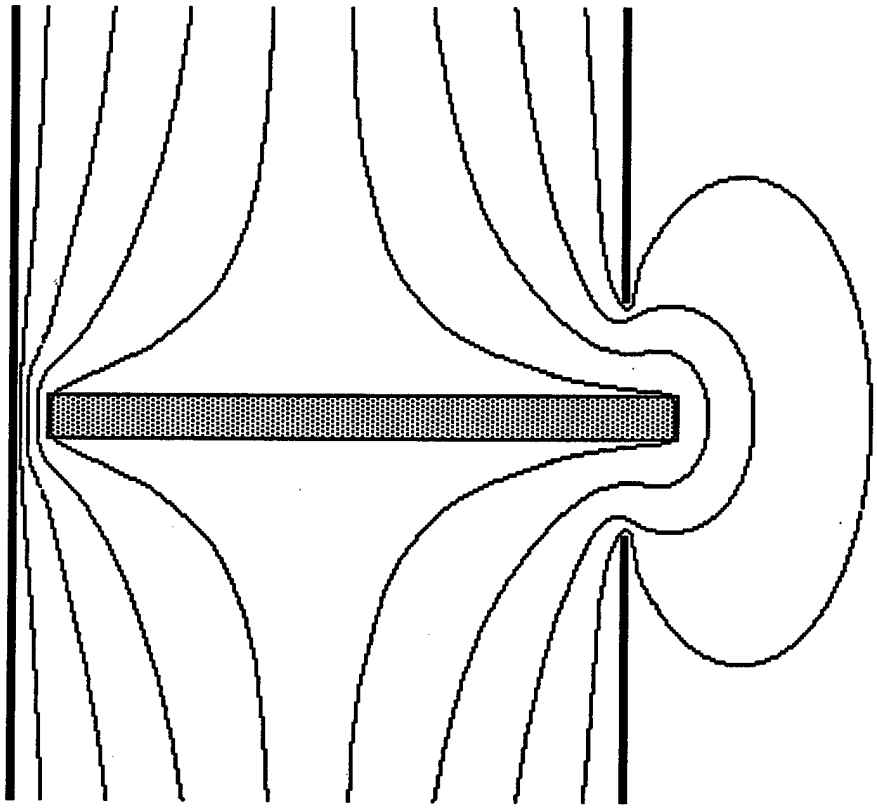

Figure 2. Magnetic Streamlines Around an Aluminum Plate.

is harmonically oscillating at a constant frequency and amplitude. The second category is the transient [14] problem, where the magnetic field pulse begins at zero, varies with time, and returns to zero at some later time. Some publications present computer programs that can solve either category of problems for many geometries. These noncommercial computer programs, however, are complicated and difficult to use. Furthermore, the utility of these programs is limited, since it is not always possible to make simplifying assumptions pertinent to the problem at hand. As an example, a general treatment of the subject would include the conductivity of the plate and the time variation of the applied magnetic field, but these features may not be necessary for this application.

These features were not included in a preliminary calculation [15], where it was assumed that the eddy current of the plate was distributed only on the surface of the plate and the magnetic field was static. To model the eddy current, the plate was covered on the top and the bottom by an array of filamentary rectangular loops. To model the condition that the magnetic induction produced by

the eddy current is equal and opposite to the coil's magnetic induction in the plate, the current in each loop was chosen to make the total magnetic induction zero at the center of each loop. Once the current in each loop was calculated, the force on each loop was found and summed to give the total force on the plate that is dependent on the inductance gradient [10],

$$F(x) = \frac{I^2 L'(x)}{2}, \tag{1}$$

where $F(x)$ is the force on the plate, I is the current in the coil, and $L'(x)$ is the inductance gradient of the coil. This calculation was repeated for a number of plate positions, and the results were compared with the inductance gradient as determined from the inductance-meter measurements. This procedure was repeated for a number of plate dimensions, plate materials, and coil designs. The calculated inductance gradients compared favorably with the measured inductance gradients in all cases, provided that the plate was a good conductor and had a thickness larger than the skin depth.

These results demonstrate that a current distribution on the surface may be a good approximation for the actual current distribution within the plate. Indeed, the actual eddy current distributions found in other simpler problems are concentrated within some depth from the surface. If this depth is small, compared to the dimensions of the plate, then this approximation can be made. The exact definition for the current depth is not known for a rectangular plate, but it can be estimated by considering a simpler problem. Let a conductor occupy all the positive x space in the three-dimensional Cartesian coordinate frame and the rest of the space be occupied by a harmonically oscillating magnetic induction in the y direction, which induces an eddy current in the conductor. The analytical solution [16] to this problem shows that the amplitudes of the magnetic induction and the eddy current decay exponentially with distance from the surface, with a decay length or "the skin depth"

$$\delta = \sqrt{\frac{2}{\mu\sigma\omega}}, \tag{2}$$

where μ is the permeability of the plate, ω is the angular frequency of the magnetic induction, and σ is the conductivity of the plate. In the present launching systems, the frequency is typically 1 kHz, ω = 6282 rad/s, and the plates are aluminum, $\sigma = 3.54 \times 10^7$ S/m. Consequently, the skin depth is

2.7 mm. This depth is small, compared to the typical length and width of the plate which are greater than 0.10 m, but it may not be small when compared to the typical plate thickness of 6 mm. The orientation of the plate relative to the magnetic induction (Figure 2) illustrates that the dimensions to be compared to the skin depth are the length or width, and not the thickness. If the skin depth were zero, in this figure, the streamlines that enter the plate at the edges would be completely expelled. Other than this, the shape of the rest of the streamlines, elsewhere, would change very little.

A zero skin depth will result if either the angular frequency ω approaches infinity, "the high-frequency limit," or if the conductivity of the material σ approaches infinity, "the super-conductor limit." In the super-conducting limit, the angular frequency can be zero, which means that the magnetic induction field can be static. This also makes the problem easier to solve but raises an interesting question: How can eddy currents be produced by a static magnetic induction field? Eddy currents are induced in a super conductor in a different manner. Consider a super conductor with no eddy currents located in a field-free region, far from the core. Now, bring the super conductor into the core where there is a magnetic induction. This motion produces the time varying magnetic induction that induces the eddy current. Thus, the time variance of the magnetic induction is implied by the condition that the magnetic induction, inside the super conductor, is zero, which means that it had to be in a field-free region at some time. Furthermore, because work must be performed to establish the eddy currents themselves, the super conductor must be pushed into the core and it will be expelled out of the core if it were released. Thus, a static magnetic field can launch a super-conducting plate, which is the "Meissner effect."

4. Eddy Current Calculations

The current loops in the preliminary calculation are now replaced by a continuous current distribution, and it is assumed that the rectangular plate has no thickness. The magnetic induction produced by an eddy current in this thin plate is given by the Biot-Savart law:

$$\vec{B}_e(\vec{x}) = \frac{1}{4\pi\mu_o}\int_{-a}^{a} dx' \int_{-b}^{b} dy' \; \frac{\vec{J}(x',y')\times(\vec{x}-\vec{x}')}{|\vec{x}-\vec{x}'|^3}, \tag{3}$$

where a is half the length and b is half the height of the plate. If the plate has infinite conductivity, then this magnetic induction, $\vec{B}_e(\vec{x})$, must be equal and opposite to the coil's magnetic induction, $\vec{B}_c(\vec{x})$, everywhere on the plate so that the total is zero everywhere in this area. This cannot be done if the coil's magnetic induction has a component in the x or y direction on the plate. When $\vec{x}-\vec{x}'$ is on the x – y plane, the cross product in the numerator has just one component in the z direction, and so $\vec{B}_e(\vec{x})$ must also be in this direction. Thus, there cannot be an x or a y component to cancel out the like components of the coil's magnetic induction. Fortunately, the plates are positioned so that these components of the coil's magnetic induction are small compared to the z component. This complication would not occur if the plate had a thickness, and the current density on all six faces of the plate were included.

The problem to be solved here is more complicated than the usual magnetostatic problem where the current density is given first and one must then find the magnetic induction everywhere. In this case, the coil's or the eddy current's magnetic induction is given first and one must then find the current density. One way to solve this problem is to assume that the current density may be approximated as a sum of terms that are products of a coefficient and a member of a set of linearly independent functions. As an example, the x component of the current distribution is assumed to be

$$J_x(x',y') = \sum_{m,n=0} A_{n,m}\, x'^n\, y'^m, \tag{4}$$

and the y component of the current distribution is assumed to be

$$J_y(x',y') = \sum_{i,k=0} C_{j,k}\, x'^j y'^k. \tag{5}$$

The set of linearly independent functions in this case consists of products of x, raised to an integer power, and y, raised to an integer power. When these functions are substituted into equation (3), the resulting integrals are analytic, and calculations are simplified (see the Appendix).

These coefficients must satisfy several conditions. First, the current density that they describe must conserve charge everywhere on the plate, or

$$\frac{\partial J_x(x',y')}{\partial x'} + \frac{\partial J_y(x',y')}{\partial y'} = 0, \tag{6}$$

for any point on the plate. Second, the current density must not cross the edges, which means that no current may enter or leave the isolated plate. Thus, $J_x(x' = a, y')$ must be zero for all points on the right edge and $J_x(x' = -a, y')$ must be zero for all points on the left edge. Similar conditions apply to the top and bottom edges, $J_y(x', y' = \pm b) = 0$. The current density vector, however, can be parallel to an edge. These conditions make some of the coefficients dependent on each other; choosing a value for one coefficient will change the value of another. It is possible to derive the relations between the coefficients, but there is another easier method to generate a physically meaningful current distribution. In this method, the current distribution is generated from another linear combination of the basic functions:

$$T(x',y') = (a^2 - x'^2)\,(b^2 - y'^2) \sum_{i,j=0}^{I,J} T_{i,j}\, x'^i\, y'^j, \tag{7}$$

where

$$J_y(x',y') = -\frac{\partial T(x',y')}{\partial x'}, \tag{8}$$

and

$$J_x(x',y') = \frac{\partial T(x',y')}{\partial y'}. \tag{9}$$

I and J in equation (7) are the maximum powers of x' and y' for the summation. Their exact values depend on the desired degree of approximation. For example, I and J were equal to 9 in the results that will be presented later.

To illustrate how equation (7) meets the conditions for a physical current distribution, consider a current distribution described by a single term,

$$T_{i,j}(x',y') = (a^2 - x'^2)(b^2 - y'^2)\, x'^i\, y'^j\, T_{i,j}, \tag{10}$$

where

$$J_x(x',y') = \frac{\partial T_{i,j}(x',y')}{\partial y'} = T_{i,j}(a^2 - x'^2)\, x'^i y'^{j-1}(jb^2 - (j+2)y'^2), \tag{11}$$

and

$$J_y(x',y') = -\frac{\partial T_{i,j}(x',y')}{\partial y'} = -T_{i,j}(b^2 - y'^2)\, x'^{i-1} y'^j (ia^2 - (i+2)x'^2). \tag{12}$$

This current distribution conserves charge and satisfies the boundary conditions at the edges for all values for i and j. Now that each term in equation (7) generates a physical current density distribution and their sum will also generate a physical current density distribution, the coefficients $T_{i,j}$ are independent from each other. When equations (11) and (12) are substituted into the Biot-Savart law, equation (3), the magnetic induction everywhere for this current distribution is

$$B_z(x,y,z)_{i,j} = \frac{T_{i,j}\mu_o}{4\pi}\int_{-a}^{a} dx' \int_{-b}^{b} dy' \frac{(y-y')(a^2-x'^2)\, x'^i y'^{j-1}(jb^2-(j+2)y'^2)}{((x-x')^2+(y-y')^2+z^2)^{3/2}}$$

$$+ \frac{T_{i,j}\mu_o}{4\pi}\int_{-a}^{a} dx' \int_{-b}^{b} dy' \frac{(x-x')(b^2-y'^2)\, x'^{i-1} y'^j (ia^2-(i+2)x'^2)}{((x-x')^2+(y-y')^2+z^2)^{3/2}}. \tag{13}$$

As stated before, all these integrals are analytic and procedures for their evaluation are given in the Appendix. The integrals in equation (13) are collected and defined as

$$I_z(x,y,z)_{i,j} = \frac{\mu_o}{4\pi}\int_{-a}^{a} dx' \int_{-b}^{b} dy' \frac{(y-y')(a^2-x'^2)x'^i y'^{j-1}(jb^2-(j+2)y'^2)}{((x-x')^2+(y-y')^2+z^2)^{3/2}}$$

$$+ \frac{T_{i,j}\mu_o}{4\pi}\int_{-a}^{a} dx' \int_{-b}^{b} dy' \frac{(x-x')(b^2-y'^2)x'^{i-1}y'^j(ia^2-(i+2)x'^2)}{((x-x')^2+(y-y')^2+z^2)^{3/2}}. \qquad (14)$$

Thus, if all the coefficients were known, then the z component of the magnetic induction of the eddy current everywhere would be

$$B_z(x,y,z) = \sum_{i,j=0}^{I,J} T_{i,j}\, I_z(x,y,z)_{i,j}. \qquad (15)$$

Similar expressions may be written for the x and y components, but they are not needed because they are zero when $z = 0$. By choosing a set of field points on the plate, it is possible to find values for the coefficients so that the magnetic induction produced by the eddy current, equation (15), is equal and opposite to the coil's magnetic induction at these points. As an example, assuming that $I = 1$ and $J = 1$, there are four unknown coefficients, $T_{0,0}$, $T_{0,1}$, $T_{1,0}$, and $T_{1,1}$, that are determined by four simultaneous equations. These equations result from making $B_z(x,y,0) = -B_c(x,y,0)$ at four points:

$$B_z(x_1,y_1,0) = -B_c(x_1,y_1,0) = T_{0,0}\, I_z(x_1,y_1,0)_{0,0} + T_{0,1}\, I_z(x_1,y_1,0)_{0,1} + T_{1,0}\, I_z(x_1,y_1,0)_{1,0} + T_{1,1}\, I_z(x_1,y_1,0)_{1,1},$$

$$B_z(x_2,y_2,0) = -B_c(x_2,y_2,0) = T_{0,0}\, I_z(x_2,y_2,0)_{0,0} + T_{0,1}\, I_z(x_2,y_2,0)_{0,1} + T_{1,0}\, I_z(x_2,y_2,0)_{1,0} + T_{1,1}\, I_z(x_2,y_2,0)_{1,1},$$

$$B_z(x_3,y_3,0) = -B_c(x_3,y_3,0) = T_{0,0}\, I_z(x_3,y_3,0)_{0,0} + T_{0,1}\, I_z(x_3,y_3,0)_{0,1} + T_{1,0}\, I_z(x_3,y_3,0)_{1,0} + T_{1,1}\, I_z(x_3,y_3,0)_{1,1},$$

$$B_z(x_4,y_4,0) = -B_c(x_4,y_4,0) = T_{0,0}\, I_z(x_4,y_4,0)_{0,0} + T_{0,1}\, I_z(x_4,y_4,0)_{0,1} + T_{1,0}\, I_z(x_4,y_4,0)_{1,0} + T_{1,1}\, I_z(x_4,y_4,0)_{1,1}. \qquad (16)$$

The exact positions of the points are arbitrary, as long as they are not on the plate's edge. Choosing the points on a uniform grid, such as the one shown in Figure 3, an example for a higher order of approximation ($I = 7$ and $J = 7$), works well. There are eight rows and columns, because the indices i and j start at 0 and continue up to and including 7, in this illustration. The resulting set of equations can be solved by using standard methods in linear algebra to find the coefficients. Because these

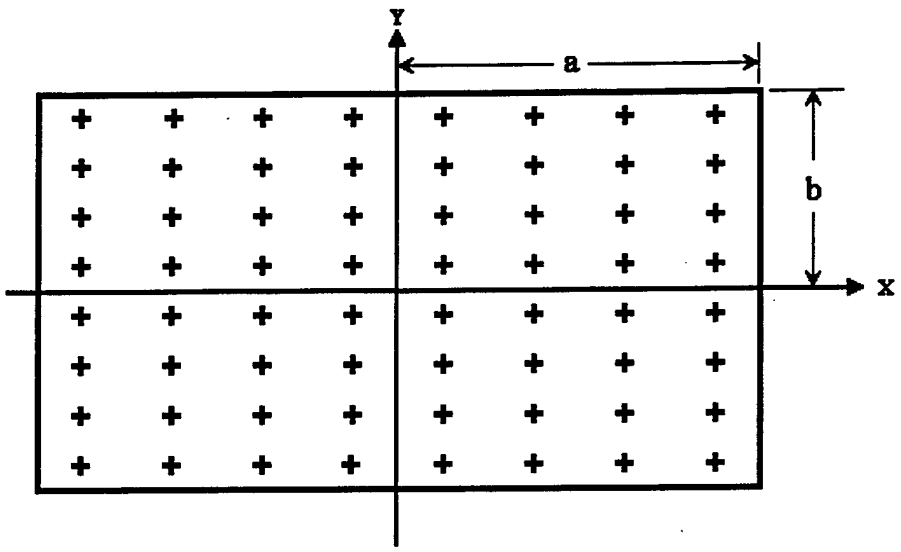

Figure 3. Grid Points Where the Total Magnetic Induction Is Zero.

points are fixed on the plate, the integrals do not change when the plate is moved away from the coil. Thus, the matrix, whose elements are the integrals, needs to be evaluated and inverted only once. The components of the vector that must be multiplied by the inverse matrix, however, are negative of the coil's magnetic induction at each point. Because these components do depend on the relative position between the coil and the plate, they must be reevaluated when the plate's position is changed.

The launch coil that will be used in the following calculations was constructed from two copper-beryllium alloy plates 15.24 × 15.24 × 0.64 cm. Each plate was milled into a square helix by a 0.64-cm-diameter end mill. The milling pattern left a conductor with cross-sectional dimensions of 0.64 × 0.64 cm in a square helix, with five complete turns. The square helixes were mounted parallel to each other, separated by 5.08 cm. The magnetic induction of the coil at the grid points was estimated by replacing the conductors with a current-carrying filament, located at the geometric center of their cross sections. Although current is actually distributed over the cross section of the bars, the magnetic induction of a distributed current approaches that of a current filament at some distance from the bar. Thus, the magnetic induction of the current-carrying filaments should be approximately the same as the coil, provided that the plate is not too close to a coil's conductor.

In Figure 4, the center of a 15- × 15-cm plate was positioned at the center of the coil. The lines within the plate are the streamlines for a current density that cancels the coil's magnetic field at 100 grid points, I = 9 and J = 9. These streamlines have the same properties as the magnetic streamlines in Figure 2. The direction of the current density is tangent to the line, and the magnitude is inversely proportional to the distance between neighboring lines. The same spacing of the streamlines at each edge of the plate indicates that the magnitudes of the current density are about the same at each edge. Because the magnitudes of the magnetic induction are also about equal at the edges, the magnitudes of the force on each edge are about equal. These forces, however, are directed toward the center of the plate, and the plate will not be accelerated out of the coil when placed in this position. In contrast, Figure 5 shows the streamlines when the plate is half way out of the coil. The streamlines are now concentrated along the back edge of the plate, indicating an area where there is a large eddy current and force on the plate, which accelerates the plate out of the coil.

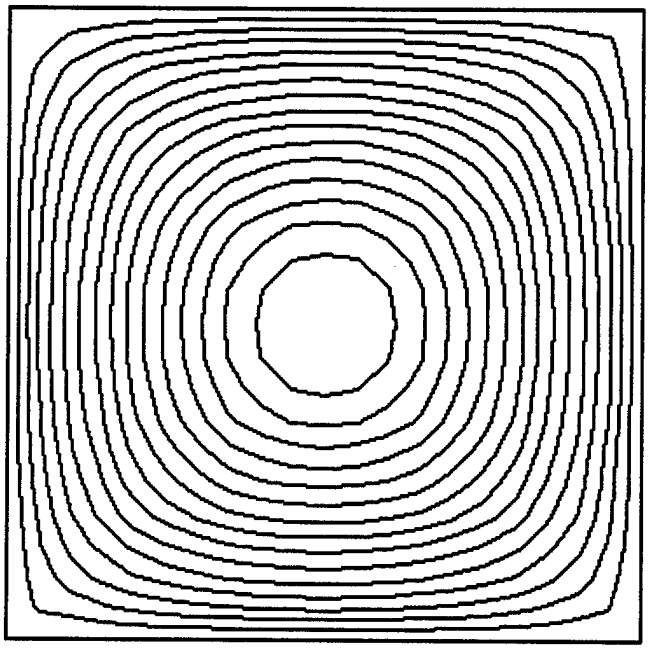

Figure 4. Current Streamlines for a Plate at the Center of the Coil.

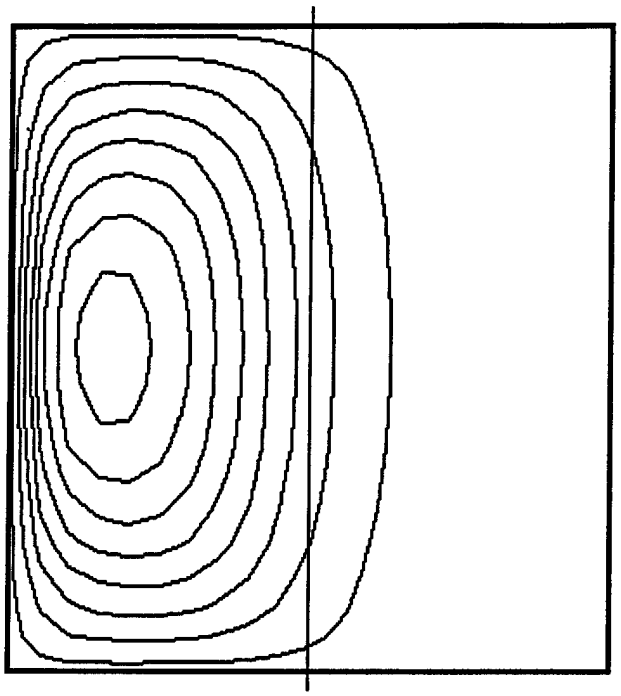

Figure 5. Current Streamlines for a Plate Half Way Out of the Coil.

Eddy currents in a plate were evident when the surface temperature distribution of a plate was observed just after it was launched in an earlier experiment [10]. The launch coil was made from a 10- × 10-cm square tube of aluminum 23-cm long with 3-mm-thick walls. Its sides were slotted so that the remaining aluminum formed a square helical coil, with nine turns. The coil was supported on the inside and outside by a stack of 5-cm-thick G10 fiberglass rectangles. The spacing between one pair of windings was widened in order to permit insertion of the metal plate into its core from the side. An aluminum plate was fabricated with a nose section that held a nail oriented along the direction of plate motion. In a low-velocity launch, the nail was driven into a plywood barrier by the plate. In this manner, the assembly was captured for viewing by an infrared (IR) video camera (8–12 μm) immediately after launch. The aluminum plate had a thick anodized coating to increase the emissivity of the surface for IR radiation. The IR video image in Figure 6a shows that the top surface of the plate was heated along its trailing and side edges. By observing the captured plate for some time with the IR video camera, we found that the time for the heat to diffuse from the edges was long, compared to the time to launch the plate. Thus, it was concluded that there was negligible

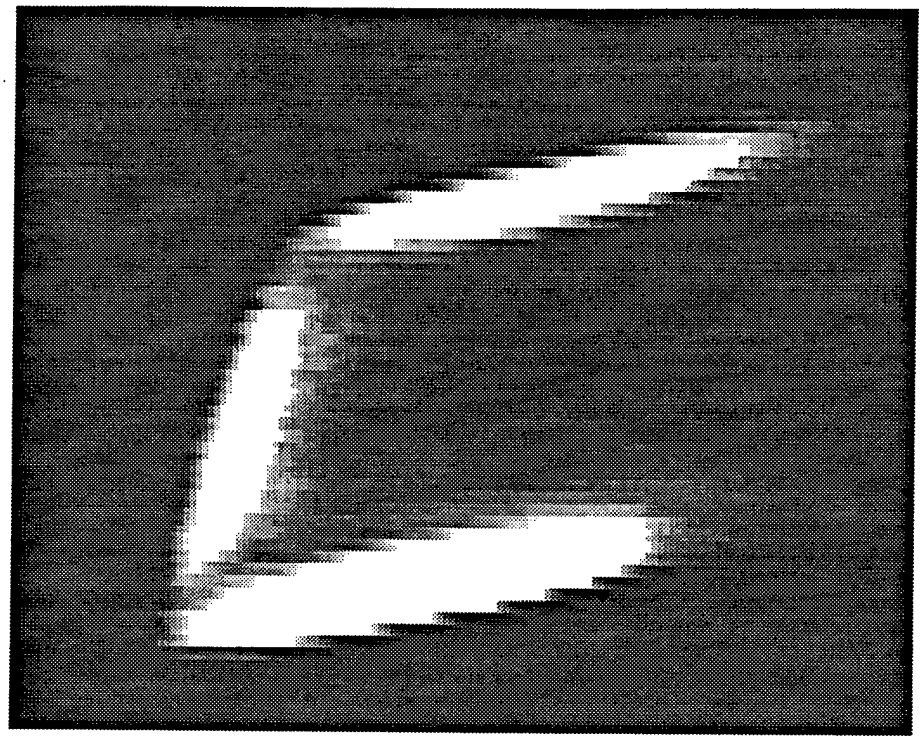

Figure 6a. IR Video Image.

heat diffusion during launch. Assuming no heat diffusion, and assuming that the conductivity of the material is independent of the temperature, the heating rate is then proportional to the square of the magnitude of the current density. The current density was calculated for the plate at its initial position inside the coil, because the plate remained close to the initial position during the entire current pulse for this low-velocity shot. The shape of the contour lines (Figure 6b), for the heating rates and the IR video image, shows that the side edges are heated by large eddy currents generated by the proximity of the coil windings. No attempt was made to correlate the heating rate with the observed intensity of the IR radiation.

5. Plate-Coil Mutual Inductance

After the current density is calculated, the mutual inductance can be found from the general expression for the energy to establish a magnetic field,

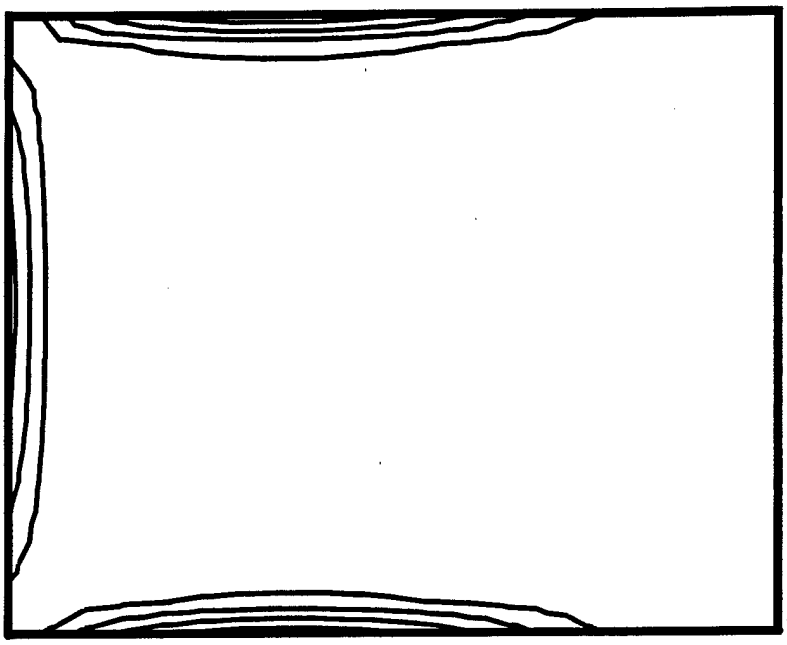

Figure 6b. Heating Rate Contour Lines.

$$W = \frac{1}{2}\int dv_c \, \vec{J}_c \cdot \vec{A} + \frac{1}{2}\int dv_p \, \vec{J}_e \cdot \vec{A}, \tag{17}$$

where J_c is the current density of the coil, J_e is the plate's current density or the eddy current, and A is the total magnetic vector potential. The first integral is taken over the volume of the coil, dv_c, and the second is taken over the volume of the plate, dv_p. When the plate is a super conductor, the total magnetic induction is zero everywhere within the volume of the plate, and the magnetic vector potential can be expressed as a gradient of a scalar function, A = grad τ. Substituting this into the last integral, it is possible to prove that the integral is zero. Thus, the energy of the magnetic field is just the first integral, provided that the plate is a super conductor. The next step is to substitute the sum for the total magnetic vector potential,

$$W = \frac{1}{2}\int dv_c \, \vec{J}_c \cdot \vec{A}_c + \frac{1}{2}\int dv_c \, \vec{J}_c \cdot \vec{A}_e. \tag{18}$$

$\vec{A}_c$ is the vector potential produced by the current density in the coil, and $\vec{A}_e$ is the vector potential produced by the eddy current in the plate. It is now possible to replace each term in this equation with an equivalent inductive element. First, start with the total magnetic energy W. If the plate is placed at some position in the coil x_0, the coil has some inductance $L(x_0)$, and if a current I were flowing through the coil, the total energy stored in the coil would be

$$W = \frac{I^2 L(x_o)}{2}. \tag{19}$$

The first integral on the right, in equation (18), represents the magnetic energy stored in the coil itself W_s, because it depends only on the coil's current density and geometry. Thus, this integral can be replaced with a similar expression,

$$W_s = \frac{I^2 L_s}{2} = \frac{1}{2}\int dv_c \, \vec{J}_c \cdot \vec{A}_c, \tag{20}$$

where L_s is the self inductance of the coil. Substituting this into equation (18), the inductance of the coil becomes

$$L(x_o) = L_s + \frac{1}{I^2}\int dv_c \, \vec{J}_c \cdot \vec{A}_e. \tag{21}$$

The integral in this equation is not in the most convenient form, because the vector potential of the eddy current is used. Although it can be calculated, it is possible to rewrite the integral in terms of quantities that have already been calculated in the course of finding the eddy current. By using the definition of the magnetic vector potential in terms of current density and some vector identities, the following identities can be proven for a coil and plate with any solid shape, each having a current density distribution:

$$\int dv_c \, \vec{J}_c \cdot \vec{A}_e = \int dv_p \, \vec{J}_e \cdot \vec{A}_c = \int dv_p \, \vec{B}_c \cdot \vec{T}, \tag{22}$$

where J = curl T. The vector T must be either zero or normal to the surface for all points on the surface. These general identities and conditions are slightly modified for the present application. The vector T has just one component in the z direction, whose curl reproduces equations (8) and (9), and it is zero at the plate's edges. In addition, only the z component of the coil's magnetic induction is used. Thus, the inductance of the coil in this application is

$$L(x_o) = L_s + \frac{1}{I^2}\int_{-a}^{a} dx \int_{-b}^{b} dy\, B_c(x,y)\, T(x,y). \tag{23}$$

Because the coil's magnetic induction and the eddy currents are proportional to the coil's current I, the inductance of the coil will be independent of I. Thus, $L(x_o)$ will depend only on the geometry.

A procedure to estimate the self-inductance of the coil L_s has been developed and presented in detail elsewhere [15], but it will be quickly described here. This procedure first divides the winding of the coil into a number of rectangular bars with different lengths and orientations. The self-inductance of the coil is then a sum of the self-inductance of each bar, and the mutual inductance between each pair of bars. The self-inductance of a bar is approximated by the geometric mean distance formula [17]. The mutual inductance between a pair of bars is approximated by replacing each bar with a filament, located at the center of the cross section of the bar, and using the exact formula for the mutual inductance between two filaments [17]. Using these approximations, and taking the appropriate sum, the self-inductance of the launch coil being considered here was calculated to be 5.90 μH. Using 5.90 μH for the self-inductance of the coil and calculating the integral in equation (23) for various plate positions, the total inductance of the coil as a function, the plate's position is shown as the upper curve in Figure 7. The lower curve is the inductance, when the measured self-inductance of the coil 5.49 μH is used instead. The diamonds in this figure are the measured inductance of the coil for various plate positions.

6. Discussion

The agreement between the lower curve and the experimental measurements in Figure 7 shows that this procedure is capable of estimating the mutual inductance between the coil and the plate. It also shows that the procedure for calculating the self-inductance of the coil gives a reasonable approximation. Therefore, it is now possible to calculate the inductance of a coil as a function of the position of a rectangular plate within it. This permits study of various coils to identify what design features will improve the efficiency of the single-stage coil gun. The results of this study will be presented in future publications.

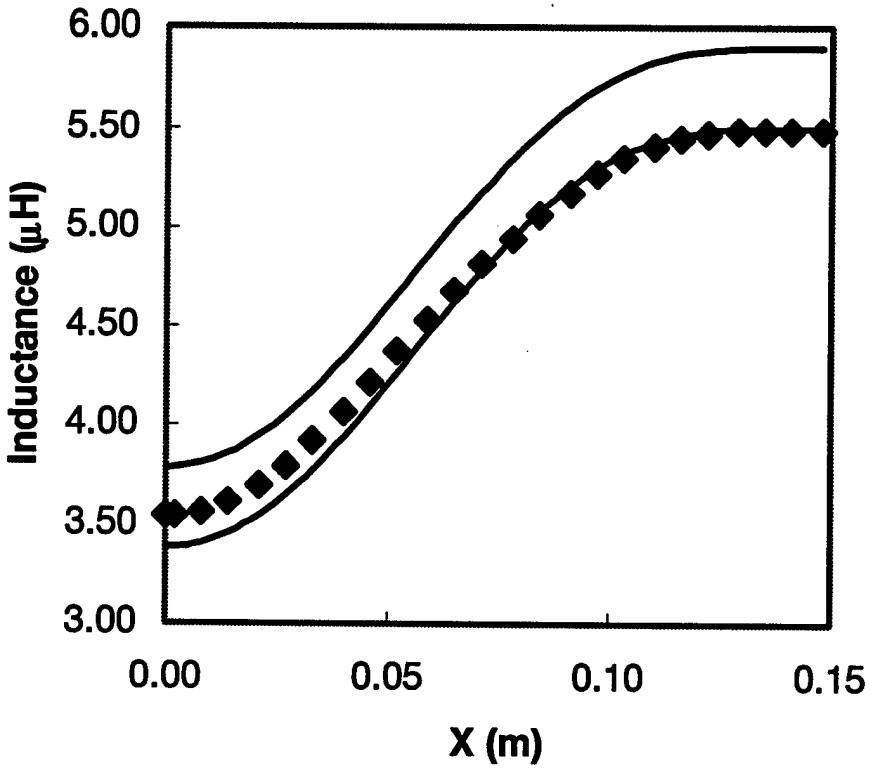

Figure 7. Calculated Coil Inductance (Solid Lines) and Measured Inductance (Diamonds).

In practice, it is found that the series expansion of the current streamline function, equation (7), is semiconvergent. When the mutual inductance of the plate and the coil for a given plate position

is calculated for increasing I and J in equation (7), the mutual inductance seems to converge to a limit, but diverges when they are made too large. This divergence may be caused by an instability in the analysis. Therefore, I and J should be kept small enough to avoid the instabilities but large enough to get reasonable results. By repeating the calculation for different "I"s and "J"s and observing when the mutual inductances start to diverge, it is possible to decide what their values should be. This instability may be indicated by the observations that the coefficients for the higher order terms do not approach a limit with increasing I and J, and the absolute values of the coefficients increase as the order of their terms increases. These features are contrary to a converging series and make it difficult or impossible to assign an error to the results.

The reason for this semiconvergence may be illustrated by applying this method to a simple analytic problem. Let the plate in Figure 3 be an infinitely long ribbon along the x-axis, with a half width b, and assume that there is a uniform magnetic field in the z direction at large distances away from the ribbon. It can be shown analytically that the current density in the ribbon is

$$J_x(y) = \frac{B_o}{\pi\mu_o} \frac{y}{\sqrt{b^2 - y^2}}, \tag{24}$$

where B_o is the magnitude of the magnetic induction. Because the current density is infinite at the edges of the ribbon, it is quite possible that there are infinite current densities at some of the edges of the rectangular plate. If this is so, polynomials of finite order are a poor approximation for the current density near these edges, since they are finite everywhere on the plate. Because the distance between these edges and the nearest grid points decreases as I and J are increased, it is possible that the higher order approximations for the current density become unstable. Had the plate, however, had a finite thickness and conductivity, then the current density should be finite everywhere. These polynomials may then be a very good approximation for the current density. Thus, this formalism is now being extended for this case, and will be the subject of future reports.

7. Conclusion

This calculation of the eddy currents and the mutual inductance depends on three assumptions: (1) the skin depth is zero, (2) the plate has zero thickness, and (3) the eddy-current density distribution in the plate can be described by a polynomial. The first assumption was made in a preliminary calculation [15] that produced very good agreement with experimental measurements. These results indicated that the skin depth may be small, compared to some dimension of the plate. After estimating the skin depth and considering the distribution of the magnetic induction around the plate, it was concluded that the skin depth should be compared with the length or the width of the plate, and not with its thickness. This calculation also demonstrated that there was a small variation in the inductance gradient, when the thickness of the plate was varied, and a plate with no thickness could be assumed. Although these first two assumptions make the problem easier to solve, they may introduce an infinite current density at some of the edges. Stickily speaking, this behavior invalidates the third assumption, because a polynomial cannot be infinite at the edges. Despite this complication, it is possible to get meaningful results with some testing and precautions.

8. References

1. Frey, R. B., G. Melani, and S. R. Stegall. "Interaction Between Kinetic Energy Penetrators and Reactive Armor." BRL-TR-2964, U.S. Army Ballistic Research Laboratory, Aberdeen Proving Ground, MD, October 1988.

2. Hackbarth, D., G. Bulmash, M. Zoltolski, M. Wilkins, and A. Kusubou. "Momentum Transfer Armor." *Proceedings 1992 Combat Vehicle Survivability Symposium*, Gaithersburg, MD, April 1992.

3. Hackbarth, D., M. Zoltoski, M. Wilkins, and A. Kusubou. "Momentum Transfer Armor." *Proceedings 1993 Combat Vehicle Survivability Symposium*, Gaithersburg, MD, April 1993.

4. Prakash, A. Private communication. U.S. Army Ballistic Research Laboratory, Aberdeen Proving Ground, MD, January 1990.

5. Prakash, A. "Simulations of Interactions Dynamics and Residual Penetration of KE Rods Impacted by Moving Plates." *Proceedings of the Second Ballistics Symposium on Classified Topics*, pp. 183–192, ADPA, Laurel, MD, 26–29 October 1992.

6. Thomson, G. M., A. Prakash, D. Showalter, and P. Plostins. Private Communications. U.S. Army Ballistic Research Laboratory, Aberdeen Proving Ground, MD, January 1990.

7. Hummer, C. R., C. E. Hollandsworth, and P. R. Berning. "Interactions Between Subscale Rods and Electromagnetically Launched Metal Plates." *Proceedings of the Third Ballistics Symposium on Classified and Controlled Topics*, ADPA, pp. 101–113, Laurel, MD, 13–15 November 1995.

8. Cowan, M. PAT-APPL-7-034 354, Filed: 6 April 1987.

9. Cowan, M., M. M. Widner, E. C. Cnare, B. W. Duggin, R. J. Kaye, and J. R. Freeman. "Exploratory Development of the Reconnection Launcher 1986–1990." *Proceedings IEEE Trans. Magnetics*, vol. 27, no. 1, pp. 563–567, January 1991.

10. Hummer, C. R., and C. E. Hollandsworth. "A Single-Stage Reconnection Gun." ARL-TR-14, U.S. Army Research Laboratory, Aberdeen Proving Ground, MD.

11. Freeman, J. R. "REGGIE, A 2-D Reconnection Gun Code." SAND88-0518, Sandia Report, Sandia National Laboratories, Albuquerque, NM, May 1988.

12. Krawczyk, A., and J. A. Tegopoulos. *Numerical Modelling of Eddy Currents*, Clarendon Press, Oxford, 1993.

13. Poltz, J., and K. Romanowski. "Solutions of Quasi-Stationary Field Problems By Means of Magnetic Scalar Potential." *IEEE Trans. on Magnetics*, vol. MAG-19, no. 6, pp. 2425–8, 1983.

14. Enokizono, M., and T. Todaka. "Three-Dimensional Eddy Current Analysis on Thin Conductors with Boundary Element Method." *IEEE Trans. on Magnetics*, vol. 28, no. 2, pp. 1655–8, 1992.

15. Berning, P. R., C. R. Hummer, C. D. Le, and W. O. Coburn. "A Theoretical and Experimental Study of the Electromagnetic Environment Surrounding a Magnetic Induction Launche." *IEEE Trans. on Magnetics*, vol. 33, no. 1, pp. 368–72, 1997.

16. Knoepfel, H. *Pulsed High Magnetic Fields*. North-Holland, Amsterdam, 1970.

17. Grover, F. W. *Inductance Calculations Working Formulas and Tables*. New York: Dover Publications, Inc., 1962.

Appendix:

Recursion Relations for the Integrals

INTENTIONALLY LEFT BLANK.

Although the integrals in equation (14) are in principle analytic, their explicit expressions quickly become long and tedious even for small i and j. In the end, however, it is their values that are required to perform the calculations. A procedure to find their values or expressions starts by identifying the general form of the integrals that appear in all of these equations, which is:

$$F(x,y,z)_{k,l} = \int_{-a}^{a} dx' \int_{-b}^{b} dy' \frac{x'^k y'^l}{((x-x')^2 + (y-y')^2 + z^2))^{3/2}}. \qquad \text{(A-1)}$$

Equation (14), for example, may be rewritten as

$$\begin{aligned} I_z(x,y,z)_{k,l} = {} & a^2 b^2 jy F(x,y,z)_{i,j-1} - a^2 jy(j+2) F(x,y,z)_{i,j+1} \\ & - b^2 yj F(x,y,z)_{i+2,j-1} + y(j+2) F(x,y,z)_{i+2,j+1} \\ & - a^2 b^2 F(x,y,z)_{i,j} + a^2 (j+1) F(x,y,z)_{i,j+2} \\ & + b^2 j F(x,y,z)_{i+2,j} - (j+2) F(x,y,z)_{i+2,j+2}. \end{aligned} \qquad \text{(A-2)}$$

Unfortunately equation (A-1) is not the final integral that must be evaluated, because the first step taken to perform the integration is to introduce a change in variables:

$$F(x,y,z)_{k,l} = \int_{x+a}^{x-a} du \int_{y+b}^{y-b} dv \frac{(x-u)^k (y-v)^l}{(u^2 + v^2 + z^2)^{3/2}}, \qquad \text{(A-3)}$$

where $u = x - x'$, $du = -dx'$, $v = y - y'$, and $dv = -dy'$. Applying the binomial theorem to the numerator,

$$(x-u)^k (y-v)^l = \sum_{n=0}^{n=k} \sum_{m=0}^{m=l} \binom{k}{n} \binom{l}{m} x^{k-n} y^{l-m} (-1)^{n+m} u^n v^m \qquad \text{(A-4)}$$

and defining a new set of integrals,

$$J(u,v)_{n,m} = \int_{x+a}^{x-a} du \int_{y+b}^{y-b} dv \frac{u^n v^m}{(u^2+v^2+z^2)^{3/2}}, \tag{A-5}$$

equation (A-3) can be rewritten as

$$F(x,y,z) = \sum_{n=0}^{n=k} \sum_{m=0}^{m=k} \binom{k}{n} \binom{l}{m} x^{k-n} y^{l-m} (-1)^{n+m} J(u,v)_{n,m}. \tag{A-6}$$

As an example, if $i = 1$ and $j = 1$, then the numerator in equation (A-3) becomes (x – u) (y – v) = xy – yu – xv + uv and the integral becomes

$$F(x,y,z)_{1,1} = xyJ(u,v)_{0,0} - yJ(u,v)_{1,0} - xJ(u,v)_{0,1} + J(u,v)_{1,1} \tag{A-7}$$

in terms of the fundamental integrals. It is implied that these fundamental integrals are evaluated at the limits of integration. In more explicit terms,

$$\begin{aligned} F(x,y,z)_{1,1} = {} & xy(J(x-a,y-b)_{0,0} - J(x-a,y+b)_{0,0} - J(x+a,y-b)_{0,0} + J(x+a,y+b)_{0,0}) \\ & - y(J(x-a,y-b)_{1,0} - J(x-a,y+b)_{1,0} - J(x+a,y-b)_{1,0} + J(x+a,y+b)_{1,0}) \\ & - x(J(x-a,y-b)_{0,1} - J(x-a,y+b)_{0,1} - J(x+a,y-b)_{0,1} + J(x+a,y+b)_{0,1}) \\ & - (J(x-a,y-1b)_{1,1} - J(x-a,y+b)_{1,1} - J(x+a,y-b)_{1,1} + J(x+a,y+b)_{1,1}). \end{aligned} \tag{A-8}$$

The value of the integral, equation (A-5), for any n and m can be found by using a set of recursion relations, which is a relationship between a higher order integral in terms of lower order integrals. These recursion relations start with the four lowest order integrals:

$$J(u,v)_{0,0} = \frac{1}{z}\arctan\frac{uv}{zr} \tag{A-9}$$

$$J(u,v)_{0,1} = -\ln(u+r), \tag{A-10}$$

$$J(u,v)_{1,0} = -\ln(v+r), \tag{A-11}$$

and

$$J(u,v)_{1,1} = -r, \tag{A-12}$$

where $r = \sqrt{u^2+v^2+z^2}$ in these equations and the ones following. The recursion relations are for $n \geq 0$ and $m \geq 2$,

$$(n+m-1)J(u,v)_{n,m} = (m-1)u^{n+1}V(u)_{m-2} - nv^{m-1}U(v)_n - (m-1)z^2 J(u,v)_{n,m-2} \tag{A-13}$$

and for $n \geq 2$ and $m \geq 0$,

$$(n+m-1)J(u,v)_{n,m} = (n-1)v^{m+1}U(v)_{n-2} - mu^{n-1}V(u)_m - (n-1)z^2 J(u,v)_{n-2,m}, \tag{A-14}$$

where $U(v)_i$ and $V(u)_j$ are the integrals,

$$U(v)_i = \int_{x+a}^{x-a} du\frac{u^i}{r} \text{ and } V(u)_j = \int_{y+b}^{y-b} dv\frac{v^j}{r}. \tag{A-15}$$

Each of these integrals have a recursion relation:

$$iU(v)_i = u^{i-1}r - (i-1)(v^2+z^2)U(v)_{i-2} \tag{A-16}$$

and

$$jV(u)_j = v^{j-1}r - (j-1)(u^2+z^2)V(u)_{j-2}, \tag{A-17}$$

where the starting integral for $U(v)_i$ are $U(v)_0 = \ln(u + r)$ and $U(v)_1 = r$, and the starting integrals for $V(u)_j$ are $V(u)_0 = \ln(v + r)$ and $V(u)_1 = r$. These recursion relations can either be used to write an explicit expression for equation (A-1), or they can be used to write a computer program, like the one listed in the next section, to calculate its value. This program does not calculate the eddy currents in the plate, but it does demonstrate how these equations are used.

```
#include <stdio.h>
#include <math.h>

/* NMAX is the absolute maximum value for nmax */
#define NMAX 20

/* MMAX is the absolute maximum value for mmax */
#define MMAX 20

struct plate {
        double a;           /* The half width of the plate        */
        double b;           /* The half height of the plate       */
        double x, y, z; /* The field point coordinates            */
    } p;

void main () {

double fxyz ( int k, int el, struct plate *p );

int k, el;

    /* Ask for and receive the half width */
    printf ("Half width = ");
    scanf ("%le", &(p.a) );

    /* Ask for and receive the half height */
    printf ("Half heigth = ");
    scanf ("%le", &(p.b) );

    /* Ask for and receive the field point */
    printf ("Field coordinate (x,y,z) = ");
    scanf ("%le %le %le", &(p.x), &(p.y), &(p.z) );

    /* Ask for and receive k */
    printf ("k = ");
    scanf ("%d", &k );
    /* Test if k is too big */
    if ( k > NMAX ) k = NMAX;

    /* Ask for and receive l */
    printf ("l = ");
    scanf ("%d", &el );
    /* Test if el is too big */
    if ( el > MMAX ) el = MMAX;
```

```
        printf ("fxyz = %e\n", fxyz ( k, el, &p ) );

} /* End of the Main program */


/* This procedure calculates the integral, equation A1                    */
double  fxyz ( int k, int el, struct plate *pd )
{

void juv ( double t[][MMAX], int n, int m, double u, double v, double z );
void poly_pow ( double *c, double x, int n);

double sum;
double xu[NMAX];
double yv[MMAX];
double capj[NMAX][MMAX];
double temp[NMAX][MMAX];

int n, m;

        /* Evaluate juv at the limits of integration */
        juv ( temp, k, el, pd->x - pd->a, pd->y - pd->b, pd->z );
        for (n = 0; n <= k; n++)
                for (m = 0; m <= el; m++) capj[n][m] = temp[n][m];

        juv ( temp, k, el, pd->x + pd->a, pd->y + pd->b, pd->z );
        for (n = 0; n <= k; n++)
                for (m = 0; m <= el; m++) capj[n][m] += temp[n][m];

        juv ( temp, k, el, pd->x - pd->a, pd->y + pd->b, pd->z );
        for (n = 0; n <= k; n++)
                for (m = 0; m <= el; m++) capj[n][m] -= temp[n][m];

        juv ( temp, k, el, pd->x + pd->a, pd->y - pd->b, pd->z );
        for (n = 0; n <= k; n++)
                for (m = 0; m <= el; m++) capj[n][m] -= temp[n][m];

        /* capj[n][m] matrix now has the values for all the fundamental */
        /* integrals, equation A5, needed to find the values for the   */
        /* integral, equation A3.
                */
        sum = 0.0;
        poly_pow ( xu, pd->x, k);       /* (x-u)^k in equation A3*/
        poly_pow ( yv, pd->y, el);      /* (y-v)^l in equation A3*/
        for ( n = 0; n <= k; n++)
```

```
                for ( m = 0; m <= el; m++ ) sum += xu[n]*yv[m]*capj[n][m];
        return sum;
}

/* Performs the integral, equation A5                              */
/* The results are stored in a temporary matrix so that they may be     */
/* added or subtracted according to the limit of integration.          */
void juv ( double t[][MMAX], int k, int el, double u, double v, double z ) {

double capu[NMAX];
double capv[MMAX];

double vz, uz, zsq;
double r;
double num, den;
double up, vp;
int i, j, n, m;
        zsq = z * z;
        vz = v*v + zsq;
        uz = u*u + zsq;
        r = sqrt ( vz + u*u );

        /* The starting values for the recursion relation, equation A16 */
        if ( u > 0.0 ) capu[0] = log(u+r);
        else capu[0] = log(vz/(r-u) ); /* An identity used when u is negative */

        capu[1] = r;

        /* The recursion relation itself, equation A16 */
        up = u;         /* up is u raised to the i-1 power     */
        for (i = 2; i <= k; i++) {
                capu[i] = (up*r - (i-1)*vz*capu[i-2])/i;
                up *= u;
        }

        /* The starting values for the recursion relation, equation A17 */
        if ( v > 0.0 ) capv[0] = log(v+r);
        else capv[0] = log( uz/(r-v) ); /*An identity used when v is negative */

        capv[1] = r;

        /* The recursion relation itself, equation A17 */
        vp = v;         /* vp is v raised to the j-1 power     */
        for (j = 2; j <= el; j++) {
                capv[j] = (vp*r - (j-1)*uz*capv[j-2])/j;
```

```
            vp *= v;
        }

        /* equation A9 */
        num = u*v;
        den = z * r;
        /* Test if z is close to zero */
        if ( fabs ( z ) < 1.0e-32 ) t[0][0] = 0.0; /* The limiting value */
        else t[0][0] = atan2 (num, den) / z;
        /* equation A10 */
        if ( u > 0.0 ) t[0][1] = -log(u+r);
        else t[0][1] = log((r-u)/vz);/* An identity used when u is negative */
        /* equation A11 */
        if ( v > 0.0 ) t[1][0] = -log(v+r);
        else t[1][0] = log((r-v)/uz);/* An identity used when v is negative */
        /* equation A12 */
        t[1][1] = -r;

        /* Use equation A13 to fill out the top row of the matrix */
        n = 0;
        for ( m = 2; m <= el; m++ )
            t[n][m] = u*capv[m-2] - zsq*t[n][m-2];
        /* Use equation A13 to fill out the second row from the top */
        n = 1;
        vp = v;
        up = u*u;
        for ( m = 2; m <= el; m++ ) {
            t[n][m] = ((m-1)*up*capv[m-2]-vp*capu[n]-(m-1)*zsq*t[n][m-2])/m;
            vp *= v;
        }
        /* Use equation A14 to fill out each column of the matrix */
        vp = v;
        for ( m = 0; m <= el; m++ ) {
            up = u;
            for ( n = 2; n <= k; n++ ) {
                t[n][m] = (n-1)*vp*capu[n-2]-m*up*capv[m]-(n-1)*zsq*t[n-2][m];
                t[n][m] /= n+m-1;
                up *= u;
            }
            vp *= v;
        }

} /* End of juv */
```

```
/* (x-u) raised to the n-th power for a given x value */

void poly_pow ( double *p, double x, int n )
{
/* The index of p[i] is the power of u or v; p[i] means u^i or v^i   */
/* The value of p[i] is the coefficient for the term                 */
/* Example: p[0] = 1.0, p[1] = -2.0, and p[2] = 1.0, would represent */
/* the polynomial 1.0 - 2.0*u + 1.0*u*u or (1-u)^2 for x = 1         */
int i;
        if ( n == 0 ) {
                p[0] = 1.0;
                return;
   }

   /* -1 raised to the n th power */
        if ( 0x0001 & n ) p[n] = -1.0;
        else p[n] = 1.0;

        for ( i = n-1; i >= 0; i--) p[i] = -x * p[i+1] * (i+1) / (n-i);
} /* End of poly_pow */
```

INTENTIONALLY LEFT BLANK.

NO. OF COPIES ORGANIZATION

2 DEFENSE TECHNICAL INFORMATION CENTER
DTIC DDA
8725 JOHN J KINGMAN RD
STE 0944
FT BELVOIR VA 22060-6218

1 HQDA
DAMO FDQ
DENNIS SCHMIDT
400 ARMY PENTAGON
WASHINGTON DC 20310-0460

1 DPTY ASSIST SCY FOR R&T
SARD TT F MILTON
RM 3EA79 THE PENTAGON
WASHINGTON DC 20310-0103

1 OSD
OUSD(A&T)/ODDDR&E(R)
J LUPO
THE PENTAGON
WASHINGTON DC 20301-7100

1 CECOM
SP & TRRSTRL COMMCTN DIV
AMSEL RD ST MC M
H SOICHER
FT MONMOUTH NJ 07703-5203

1 PRIN DPTY FOR TCHNLGY HQ
US ARMY MATCOM
AMCDCG T
M FISETTE
5001 EISENHOWER AVE
ALEXANDRIA VA 22333-0001

1 PRIN DPTY FOR ACQUSTN HQ
US ARMY MATCOM
AMCDCG A
D ADAMS
5001 EISENHOWER AVE
ALEXANDRIA VA 22333-0001

1 DPTY CG FOR RDE HQ
US ARMY MATCOM
AMCRD
BG BEAUCHAMP
5001 EISENHOWER AVE
ALEXANDRIA VA 22333-0001

NO. OF COPIES ORGANIZATION

1 INST FOR ADVNCD TCHNLGY
THE UNIV OF TEXAS AT AUSTIN
PO BOX 202797
AUSTIN TX 78720-2797

1 USAASA
MOAS AI W PARRON
9325 GUNSTON RD STE N319
FT BELVOIR VA 22060-5582

1 CECOM
PM GPS COL S YOUNG
FT MONMOUTH NJ 07703

1 GPS JOINT PROG OFC DIR
COL J CLAY
2435 VELA WAY STE 1613
LOS ANGELES AFB CA 90245-5500

1 ELECTRONIC SYS DIV DIR
CECOM RDEC
J NIEMELA
FT MONMOUTH NJ 07703

3 DARPA
L STOTTS
J PENNELLA
B KASPAR
3701 N FAIRFAX DR
ARLINGTON VA 22203-1714

1 US MILITARY ACADEMY
MATH SCI CTR OF EXCELLENCE
DEPT OF MATHEMATICAL SCI
MDN A MAJ DON ENGEN
THAYER HALL
WEST POINT NY 10996-1786

1 DIRECTOR
US ARMY RESEARCH LAB
AMSRL CS AL TP
2800 POWDER MILL RD
ADELPHI MD 20783-1145

1 DIRECTOR
US ARMY RESEARCH LAB
AMSRL CS AL TA
2800 POWDER MILL RD
ADELPHI MD 20783-1145

NO. OF
COPIES ORGANIZATION

3 DIRECTOR
US ARMY RESEARCH LAB
AMSRL CI LL
2800 POWDER MILL RD
ADELPHI MD 20783-1145

ABERDEEN PROVING GROUND

4 DIR USARL
AMSRL CI LP (305)

NO. OF COPIES	ORGANIZATION
2	INST FOR ADVNCD TCHNLGY THE UNIV OF TEXAS AT AUSTIN IAN MCNAB SID PRATAP PO BOX 202797 AUSTIN TX 78720-2797
	ABERDEEN PROVING GROUND
42	DIR USARL AMSRL SE R H WALLACE AMSRL SL P TANENBAUM AMSRL WM T W MORRISON AMSRL WM TA W BRUCHEY G FILBEY W GILLICH T HAVEL M KEELE AMSRL WM TC R COATES W DE ROSSET R MUDD AMSRL WM TD A DIETRICH K FRANK AMSRL WM TB R FREY AMSRL WM TE P BERNING J CORRERI D DANIEL C HOLLANDSWORTH C HUMMER (5 CP) L KECSKES T KOTTKE K MAHAN M MCNEIR A NIILER J POWELL A PRAKASH S ROGERS H SINGH C STUMPFEL G THOMSON

NO. OF COPIES	ORGANIZATION
	AMSRL WM M R BOSSOLI S CORNELISON F PIERCE AMSRL WM BD P KASTE AMSRL WM BE G KATULKA K WHITE AMSRL WM BC P WEINACHT A ZIELINSKI

INTENTIONALLY LEFT BLANK.

REPORT DOCUMENTATION PAGE

Form Approved
OMB No. 0704-0188

1. AGENCY USE ONLY *(Leave blank)*	2. REPORT DATE	3. REPORT TYPE AND DATES COVERED
	March 1998	Final, August 1996 - 1997

4. TITLE AND SUBTITLE

Mutual Inductance Between a Coil and an Electromagnetically Launched Plate

5. FUNDING NUMBERS

1L162618AH80

6. AUTHOR(S)

Charles R. Hummer and Paul R. Berning

7. PERFORMING ORGANIZATION NAME(S) AND ADDRESS(ES)

U.S. Army Research Laboratory
ATTN: AMSRL-WM-TE
Aberdeen Proving Ground, MD 21005-5066

8. PERFORMING ORGANIZATION REPORT NUMBER

ARL-TR-1643

9. SPONSORING/MONITORING AGENCY NAMES(S) AND ADDRESS(ES)

10.SPONSORING/MONITORING AGENCY REPORT NUMBER

11. SUPPLEMENTARY NOTES

12a. DISTRIBUTION/AVAILABILITY STATEMENT

Approved for public release; distribution is unlimited.

12b. DISTRIBUTION CODE

13. ABSTRACT *(Maximum 200 words)*

A possible countermunition against kinetic energy (KE) rods is a thin square metal launched edge-on so that an edge strikes the rod first followed by the rest of the plate. A properly designed coil gun can launch plates edge-on to velocities of several hundred meters per second. The proper design of the coil gun depends on knowing the mutual inductance between the coil and the plate, which was calculated by assuming that the current distribution in plate can be described by a polynomial that has some arbitrary coefficients. These coefficients were determined by equating the magnetic induction of the current distribution to the negative of the applied magnetic induction of the launch coil at selected points on the plate. This step was aided by the fact that all the integrals arising from the Biot-Savart law are analytic. In the next step, the mutual inductance was calculated from the current distribution and the applied magnetic induction. The calculation was repeated for various plate positions in the coil. These results were used to design the power supply for the launch coil and to calculate the final velocity of the plate.

14. SUBJECT TERMS	15. NUMBER OF PAGES
coil gun, inductance calculation, electromagnetic launcher	39
	16. PRICE CODE

17. SECURITY CLASSIFICATION OF REPORT	18. SECURITY CLASSIFICATION OF THIS PAGE	19. SECURITY CLASSIFICATION OF ABSTRACT	20. LIMITATION OF ABSTRACT
UNCLASSIFIED	UNCLASSIFIED	UNCLASSIFIED	UL

INTENTIONALLY LEFT BLANK.

USER EVALUATION SHEET/CHANGE OF ADDRESS

This Laboratory undertakes a continuing effort to improve the quality of the reports it publishes. Your comments/answers to the items/questions below will aid us in our efforts.

1. ARL Report Number/Author ARL-TR-1643 (Hummer) Date of Report March 1998

2. Date Report Received _____

3. Does this report satisfy a need? (Comment on purpose, related project, or other area of interest for which the report will be used.) _____

4. Specifically, how is the report being used? (Information source, design data, procedure, source of ideas, etc.) _____

5. Has the information in this report led to any quantitative savings as far as man-hours or dollars saved, operating costs avoided, or efficiencies achieved, etc? If so, please elaborate. _____

6. General Comments. What do you think should be changed to improve future reports? (Indicate changes to organization, technical content, format, etc.) _____

CURRENT ADDRESS

Organization

Name E-mail Name

Street or P.O. Box No.

City, State, Zip Code

7. If indicating a Change of Address or Address Correction, please provide the Current or Correct address above and the Old or Incorrect address below.

OLD ADDRESS

Organization

Name

Street or P.O. Box No.

City, State, Zip Code

(Remove this sheet, fold as indicated, tape closed, and mail.)

(DO NOT STAPLE)

DEPARTMENT OF THE ARMY

OFFICIAL BUSINESS

NO POSTAGE
NECESSARY
IF MAILED
IN THE
UNITED STATES

BUSINESS REPLY MAIL
FIRST CLASS PERMIT NO 0001,APG,MD

POSTAGE WILL BE PAID BY ADDRESSEE

DIRECTOR
US ARMY RESEARCH LABORATORY
ATTN AMSRL WM TE
ABERDEEN PROVING GROUND MD 21005-5066